Comments on Inorganic Chemistry
Publication details, including instructions for authors and subscription information:
http://www.informaworld.com/smpp/title~content=t713455155

The Structural Role of Metal-Organonitrogen Subunits in the Molecular Manipulation of Molybdenum Oxides

Douglas Hagrman[a]; Pamela J. Hagrman[a]; Jon Zubieta[a]
[a] Department of Chemistry, Syracuse University, Syracuse, NY

To cite this Article Hagrman, Douglas , Hagrman, Pamela J. and Zubieta, Jon(1999) 'The Structural Role of Metal-Organonitrogen Subunits in the Molecular Manipulation of Molybdenum Oxides', Comments on Inorganic Chemistry, 21: 4, 225 — 261
To link to this Article: DOI: 10.1080/02603599908012008
URL: http://dx.doi.org/10.1080/02603599908012008

The Structural Role of Metal-Organonitrogen Subunits in the Molecular Manipulation of Molybdenum Oxides

DOUGLAS HAGRMAN, PAMELA J. HAGRMAN
and JON ZUBIETA*
Department of Chemistry,
Syracuse University,
Syracuse, NY 3244–4100

(Received March 20, 1999)

Although solid state metal oxides are of both fundamental and practical interest, the designed synthesis of such materials remains an elusive goal. However, valuable synthetic guidelines may be derived from a consideration of the plethora of Nature's remarkable materials which contain composites of molecules or microstructures in which inorganic components coexist with organic components. The presence of organic subunits can profoundly influence the crystallization of the inorganic microstructure, offering a powerful tool for the design of novel materials. In the specific case of molybdenum oxide phases, metal-organoamine molecules, fragments, an even polymeric coordination complex cations may be exploited in the self-assembly of complex hierarchical materials.

Keywords: *Molybdenum oxide solids; organic templates; metal-organoamine polymeric complexes; hydrothermal synthesis; organic-inorganic hybrid materials*

* Correspondence Author.

Comments Inorg. Chem.
1999, Vol. 21, No. 4-6, pp. 225-261
Reprints available directly from the publisher
Photocopying permitted by license only

INTRODUCTION

Among the inorganic materials enjoying widespread contemporary interest, the metal oxide based solid phases occupy a prominent position by virtue of their applications to catalysis, sorption, molecular electronics, energy storage, optical materials and ceramics.[1–7] The diversity of properties associated with these materials reflects the chemical composition, which allows variations in covalency, geometry and oxidation states, and the crystalline architecture, which may provide different pore structures, coordination sites, or juxtapositions of functional groups.

However, the design of the structures of such materials remains a challenge in solid state chemistry. While organic materials have been synthesized which self-assemble into ordered arrays at low temperature and which exhibit molecular recognition and biomimetic activity, the ability to synthesize inorganic materials by rational design remains elusive. Small, soluble molecular building blocks with well-defined reaction chemistries which allow their low-temperature assembly into crystalline solid state inorganic materials are not well known, and the temperatures conventionally used in solid state synthesis result in dissociation of potential coordination complex building blocks in route to a thermodynamic phase. On the other hand, the ubiquity of inorganic oxide phases in both the geosphere and the biosphere[8–10] suggests that naturally occurring oxides may provide useful guidelines for the preparation of synthetic phases and the modification of oxide microstructures. It is now appreciated that small amounts of organic material can have a profound influence on the growth of inorganic oxides. Not only the typical morphology of the oxide, but even the polymorph adopted by the material may be controlled by the presence of an organic component. Organisms use organic material to control the nucleation and growth of inorganic minerals. For example, the trigonal structure of SiO_2 can be directed to a plethora of widely varying habits by various organisms. The aragonite or calcite forms of $CaCO_3$ can be specifically nucleated by molluscs. Furthermore, in contrast to these dense phases, organic materials can be incorporated stoichiometrically into the inorganic frameworks in the synthesis of zeolites and other hybrid materials.

This approach to the synthesis of oxides exploits the synergism between organic and inorganic components in the sense that the organic component serves to imprint some structural information onto the inorganic network. There is thus a hierarchical coding of the chemistry and

crystal growth. This approach requires a shift in synthetic paradigm from the thermodynamic to the kinetic regime in which equilibrium phases are replaced by higher order architectures of consolidated matter. One consequence of this approach is the need to adopt the techniques of *chemie douce*[11] or intermediate-temperature synthesis since complex hierarchical materials will decompose at the elevated temperatures of conventional solid state synthesis. The general approach that has been adopted employs organic materials at low temperature to modify or control the surface of growing oxide crystals in a hydrothermal medium.

There are now four major classes of oxides in which organic constituents play a major structure-directing role: zeolites,[12] biomineralized materials,[13] mesoporous oxides of the MCM-41 class'4 and transition metal phosphates with entrained organic cations.[15] We have begun to elaborate a fifth class of such materials, namely, organoamine-molybdenum oxide hybrid phases.[16,17] A subclass of this group exploits a secondary transition metal center to link the molybdenum oxide subunits, to provide charge compensation, or as a component of coordination complex polymer cation which provides a matrix for the molybdenum oxide substructure.

GENERAL SYNTHETIC CONSIDERATIONS

Hydrothermal Synthesis

Although well-established for the preparation of aluminosilicates, hydrothermal techniques[18] have only recently been adopted for the preparation of a wide variety of metastable materials, including transition metal phosphates, metal organophosphonates, and complex polyoxoalkoxometalates.[19] Hydrothermal reactions are typically carried out in the temperature range.20–260 °C under autogenous pressure, so as to exploit the self-assembly of the product from soluble precursors. The reduced viscosity of water under these conditions enhances diffusion processes so that solvent extraction of solids and crystal growth from solution are favored. Since differential solubility problems are minimized, a variety of simple precursors may be introduced, as well as a number of organic and/or inorganic structure-directing agents from which those of appropriate size and shape may be selected for efficient

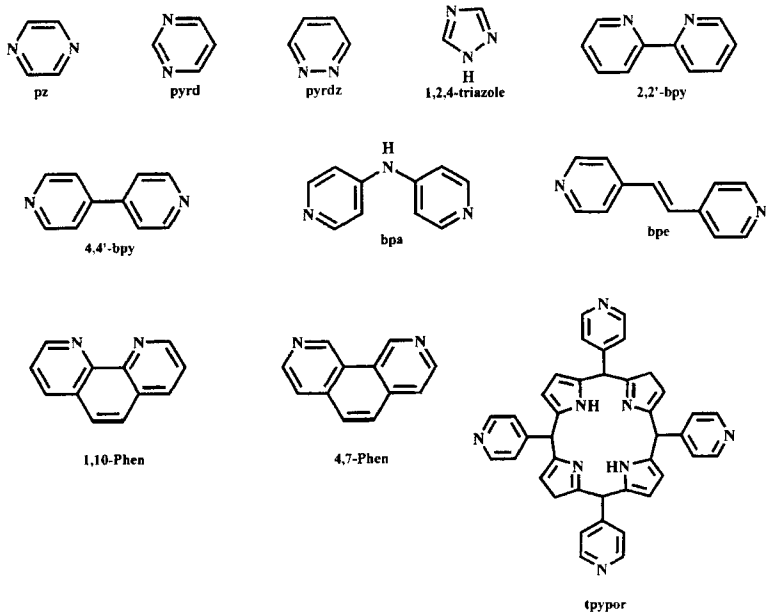

FIGURE 1 Representative organonitrogen ligands of this study

crystal packing during the crystallization process. Under such nonequilibrium crystallization conditions, metastable kinetic phases rather than the thermodynamic phase are most likely isolated. While several pathways, including that resulting in the most stable phase, are available in such nonequilibrium mixtures, the kinetically favored structural evolution results from the smallest perturbations of atomic positions. Consequently, nucleation of a metastable phase may be favored.

Synthetic Building Blocks

The syntheses proceed from the self-assembly of three component building blocks: a di- or multi-topic organoamine ligand, a first row transition metal cation and a molybdate source. While organoamine constituents have been conventionally introduced as charge-balancing counterions in zeolite synthesis, in our application the organic compo-

nent serves as a ligand to the secondary metal site, the first row transition or post-transition metal cation. Consequently, a coordination complex cation is assembled which serves to provide charge-compensation, space-filling and structure-directing roles.

The structure of the organoamine-secondary metal complex cation is derived, of course, from the geometrical requirements of the ligand as well as the coordination preferences of the metal.[20] As illustrated in Figure 1, the ligand set may include chelating agents which coordinate to a single metal center or bridging ligands of various extensions which may provide a polymeric cationic scaffolding for the entraining of the molybdenum oxide substructure. One strategy adopts appropriate stoichiometric control to form mononuclear metal-ligand chelate complex cations $\{M(N\ N)_2\}^{n+}$ which are coordinatively unsaturated and hence capable of bonding to the oxo-groups of the molybdate substructure, so as to provide linkage between the oxide subunits. Alternatively, a ligand which adopts a bridging modality between secondary metal sites will provide a one-, two- or three-dimensional matrix for the modification of the oxide structure, as shown in Figure 2.

The properties of this cationic component may be tuned by exploiting the preferred coordination modes of various transition and post-transition metal cations. For example, while a Cu(II)-organoamine fragment will likely exhibit 4+2 or 4+1 coordination geometries, the Cu(I) counterpart will result in low coordination numbers with tetrahedral or trigonal planar geometries preferred. Similarly, a Ni(II)-based cation will adopt more regular octahedral coordination, while Zn(II) species may adopt various coordination modes.

The nature of the molybdenum oxide component can be directed to some extent by the choice of reaction conditions. Thus, while low pH (3 to 5), short reaction times (10–48 h), and lower temperature ranges (110–160 °C) favor the formation of molybdate clusters as structural building blocks, conditions of higher pH (5 to 8) and more extreme temperatures and exposure times generally result in architectures in which the secondary metal is incorporated into a bimetallic oxide network and/or in which the molybdate cluster identity is lost upon fusing into one- or two-dimensional molybdenum oxide substructures. We will illustrate these approaches and characteristic features with a discussion of representative structural variants.

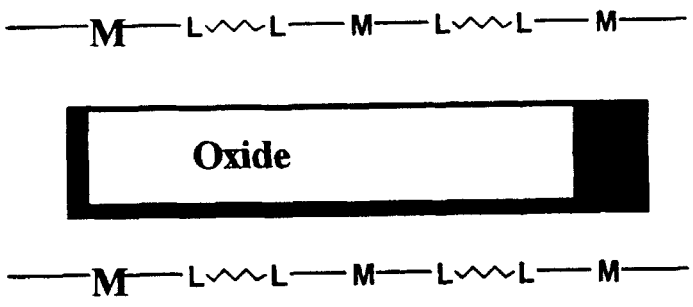

(a)

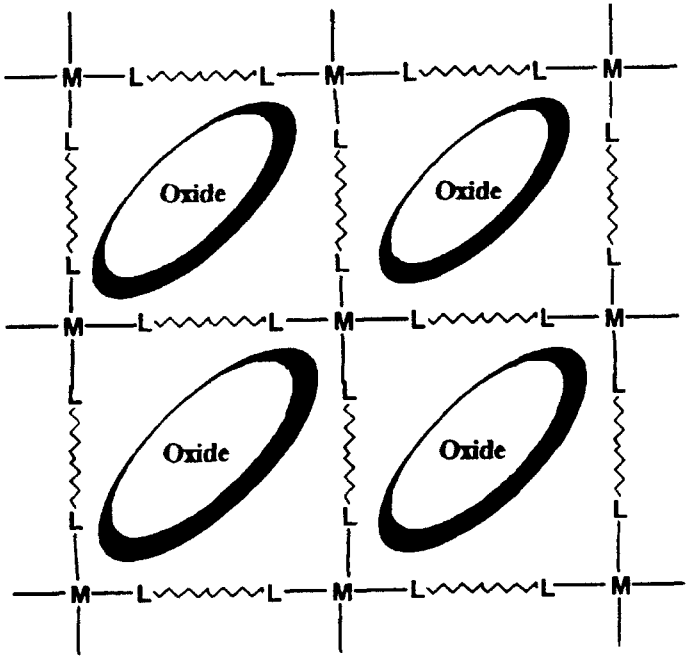

(b)

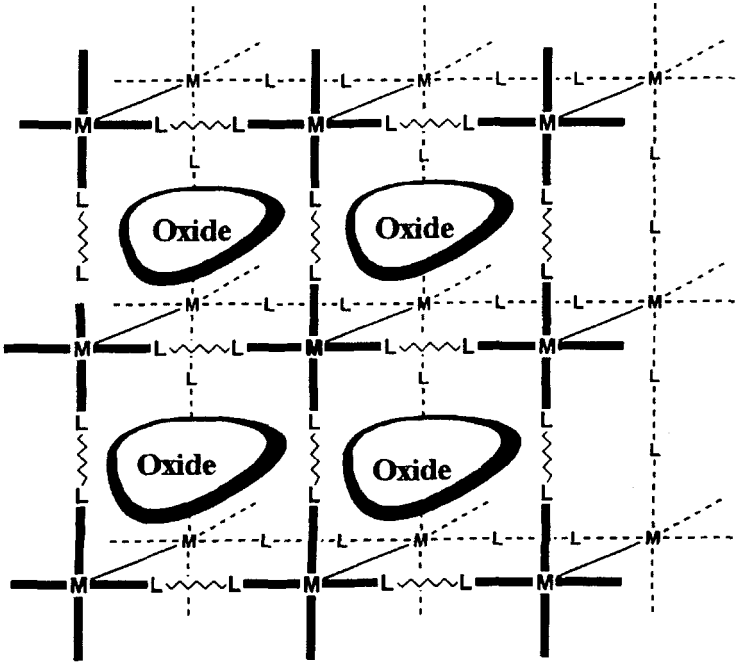

(c)

FIGURE 2 Schematic representations of the roles of ditopic organonitrogen ligands in the construction of one-, two- and three-dimensional coordination complex cation polymers for the entraining and structural modification of molybdenum oxide substructures

STRUCTURAL CHEMISTRY OF METAL-ORGANONITROGEN-MOLYBDENUM OXIDE PHASES

The discussion will focus on two types of molybdenum oxides: (i) those with distinctly molecular architectural subunits, namely, polyoxomolybdate clusters and molecular metal-organonitrogen complex cations; and (ii) those with coordination complex polymeric cations and a variety of molybdenum oxide subunits.

The structural prototype for this class of materials is provided by this molecular species[{Cu(*o*-phen)$_2$}$_2$Mo$_8$O$_{26}$](**1**),[21] shown in Figure 3. The structure consists of an α-octamolybdate unit [Mo$_8$O$_{26}$]$^{4-}$ decorated by peripheral {Cu(*o*-phen)$_2$}$^{2+}$ groups, each coordinated to a terminal oxo-group of an octahedral molybdate unit in the girdle of edge-sharing octahedra defining the cluster equator. The structure of **1** establishes that the peripheral oxo-groups of the cluster are sufficiently basic to coordinate to oxophilic metal complex units, suggesting that less sterically demanding ligands about the copper site could allow the Cu(II)-organonitrogen unit to bridge molybdate fragments.

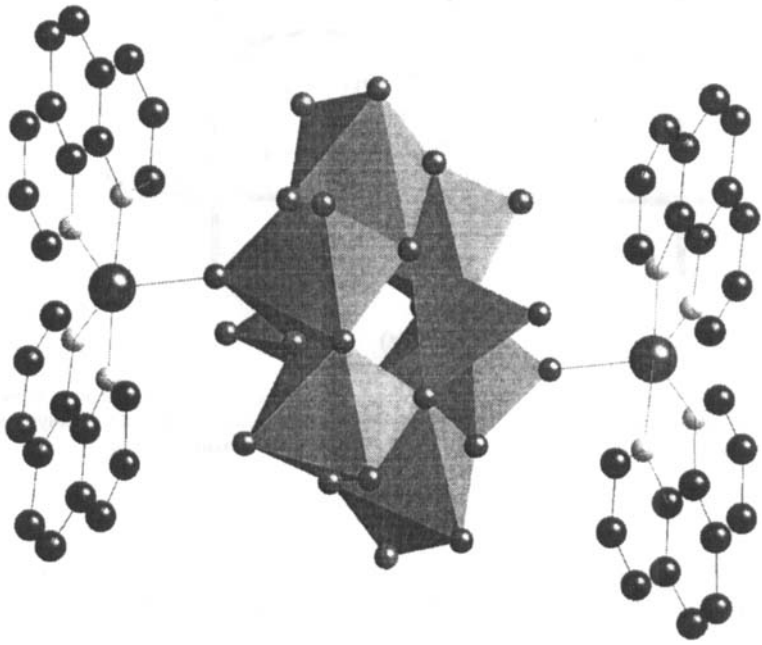

FIGURE 3 A view of the structure of [{Cu(o-phen)$_2$}$_2$Mo$_8$O$_{26}$] (1)

This expectation was realized with the isolation of [{Cu(en)$_2$}$_2$ Mo$_8$O$_{26}$] (**2**),[22] shown in Figure 4. The structure consists of γ–octamolybdate clusters linked through {Cu(en)$_2$}$^{2+}$ complexes into a virtual

two-dimensional network. The Cu(II) site exhibits 4 + 2 coordination geometry $\{CuN_4O_2\}$ with the oxo-groups occupying the axial positions with elongated Cu-O bond distances.

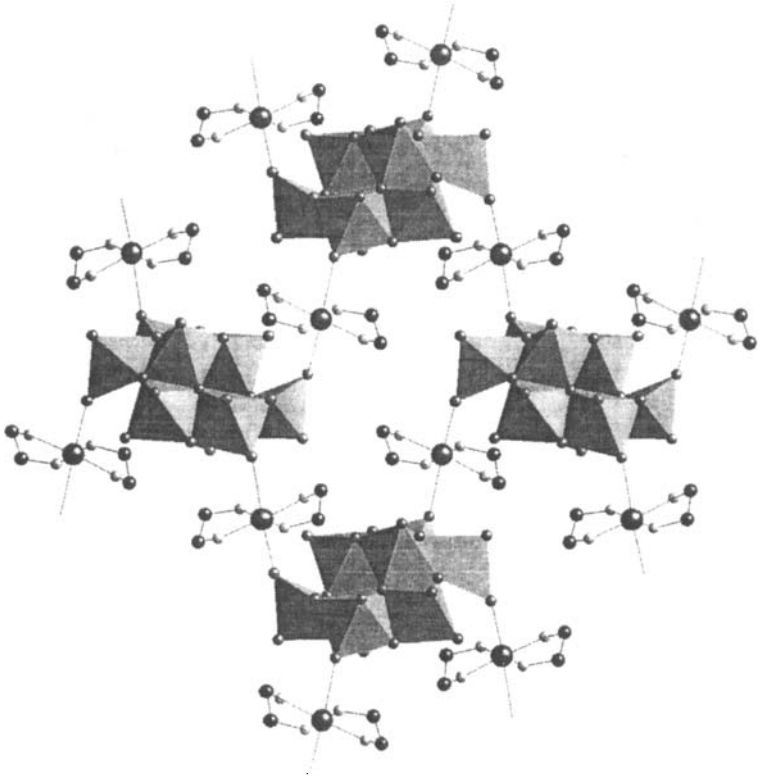

FIGURE 4 A view of the two-dimensional networks of $[\{Cu(en)_2\}_2Mo_8O_{26}]$ (**2**)

It is noteworthy that compound **2** exhibits the γ-form of the octamolybdate, while **1** displays the α-form. To date, five isomers of $[Mo_8O_{26}]^{4-}$ have been described, as shown in Figure 5. The α-, β and γ-forms have been isolated in a number of salts while the 6-form has been previously described as the (α-δ) or (β–δ) intermediate structure.[23–25] As we shall see, the ε-form is thus far unique to the composite solids of this study. These isomeric structures differ in the number, types

and connectivities of the constituent molybdenum polyhedra. The five forms are interrelated by minimal bond breaking though lengthening of weak axial interactions and rotations of the polyhedra. Since there are relatively small energy differences between these structural types, the occurrence of a particular isomer in the hydrothermal product is not predictable.

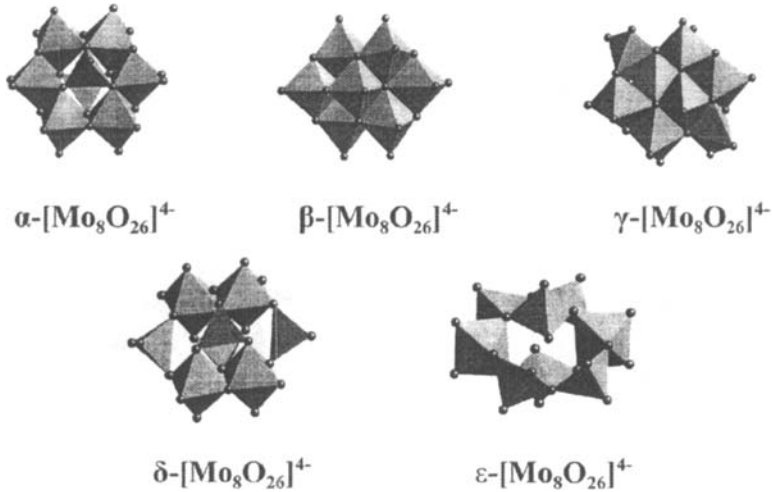

FIGURE 5 Polyhedral representations of the structures of the α, β, γ, δ, and ε-forms of $[Mo_8O_{26}]^{4-}$

The structural role of the secondary metal may also be significant, a characteristic illustrated by the structure of $[\{Ni(2,2'\text{-bpy})_2\}_2Mo_8O_{26}]$ (**3**).[26] As shown in Figure 6, the structure consists of β–$[Mo_8O_{26}]^{4-}$ subunits linked by $\{Ni(2,2'\text{-bpy})_2\}^{2+}$ fragments into a one-dimensional chain. In contrast to the Jahn-Teller distorted geometries of the Cu(II) prototypes, the Ni(II) centers enjoy normal bond distances to the oxo-groups of the molybdate clusters and cis-linkage in bridging adjacent cluster sites.

The influence of ligand geometry, in the sense of the juxtaposition of donor groups, is illustrated by the structure of $[\{Cu_3(4,7\text{-phen})_3\}_2Mo_{14}O_{45}]$ (**4**).[27] While the relative disposition of the nitrogen donors of the ligand precludes chelation, the orientation is admirably suited to the formation of planar trinuclear cationic subunits. Thus, in the presence of

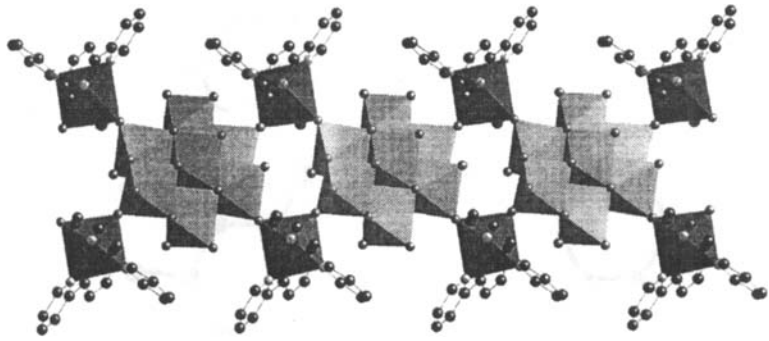

FIGURE 6 The structure of $[\{Ni(2,2'\text{-bpy})_2\}_2Mo_8O_{26}]$ (**3**)

Cu(I), the trinuclear cation $\{Cu_3(4,7\text{-phen})_3\}^{3+}$ is formed as the cationic substructure, shown in Figure 7a. A most curious feature of the structure is the presence of two distinct cluster submotifs, $[Mo_6O_{19}]^{2-}$and β-$[Mo_8O_{26}]^{4-}$, which are linked through bonding to the cations into a two-dimensional network, shown in Figure 7b. The hexamolybdate subunit is effectively sandwiched between two cationic clusters as illustrated in Figure 7c.

The consequences of subtle changes in reaction conditions can also be quite dramatic. For example, increasing reaction times and raising the pH to 6–7 results in a material in which the molybdate cluster subunits have fused into a one-dimensional chain, $[\{Cu(2,2'\text{-bpy})\}_2Mo_8O_{26}]$ (**5**),[28] shown in Figure 8. The structure may be described as a one-dimensional molybdate chain constructed from edge- and corner- sharing $\{MoO_6\}$ octahedra and decorated with peripheral $\{Cu(bpy)\}^{2+}$ groups. The Cu(II) site adopts distorted square pyramidal geometry $\{CuN_2O_3\}$ while bridging three $\{MoO_6\}$ octahedra. Inspection of the molybdate chain reveals that it is constructed of δ-$[Mo_8O_{26}]^{4-}$ fragments linked so as to expand the coordination of the five-coordinate sites of the free clusters through bridging oxo-groups, highlighted in the figure.

Coordination Complex Cation Polymers As Building Blocks

Another strategy for the modification of oxide structure exploits the use of coordination complex polymers as a cationic scaffolding, an

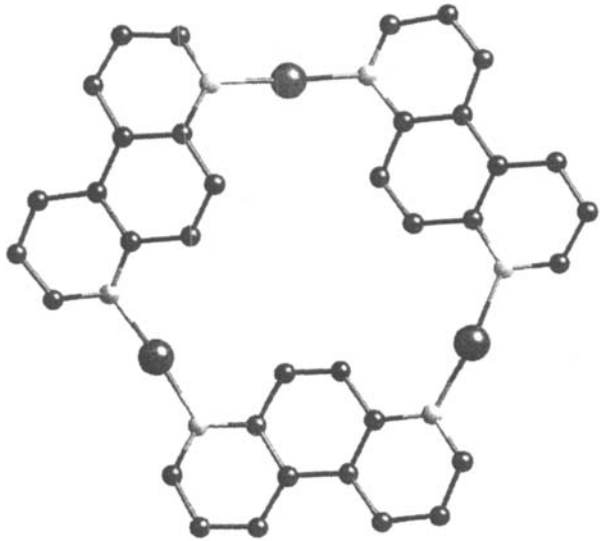

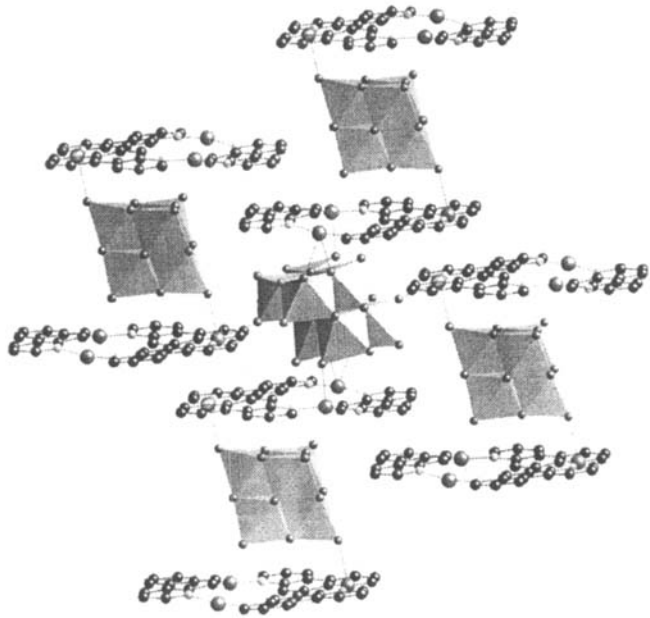

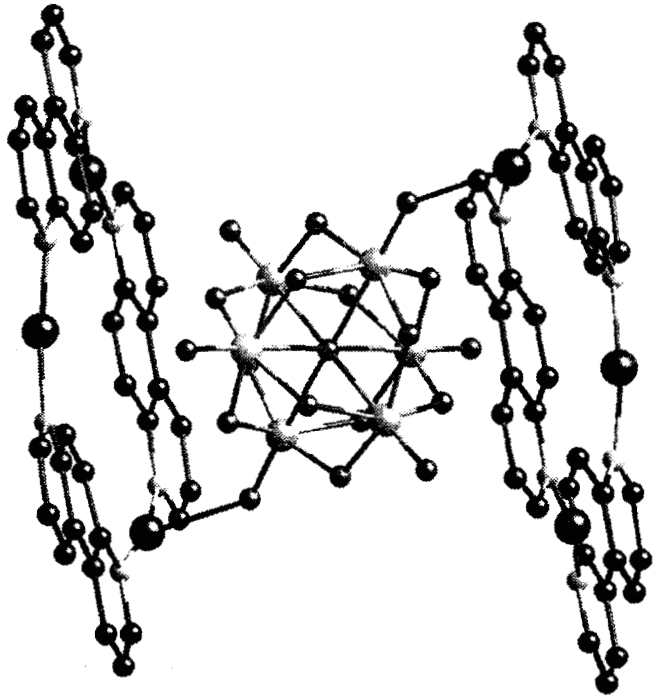

FIGURE 7 (a) A view of the structure of the trinuclear cationic motif, $\{Cu_3(4,7\text{-phen})_3\}^{3+}$, of **4**. (b) The two-dimensional network constructed from β-$[Mo_8O_{26}]^{4-}$, $Mo_6O_{19}]^{2-}$, and $\{Cu_3(4,7\text{-phen})_3\}^{3+}$ subunits. (c) The $[\{Cu_3(4,7\text{-phen})_3\}_2(Mo_6O_{19})]^{4+}$ unit

approach inspired by recent advances in the crystal engineering of coordination polymers.[29] The synthesis exploits appropriate metal centers linked through suitable polydentate ligands for the self-assembly of extended networks. Polyfunctional rod-like ligands such as 4,4'-bipyridine provide tethers for the construction of solids with diverse topologies. Such polymeric scaffolding $\{M(N\text{-linker-}N)_x\}^{n+}$, can provide a matrix of variable channel dimensions for imprinting structural information on the oxide component. We naively anticipated that the structure of this oxide component would conform to the constraints imposed by the cationic skeleton.

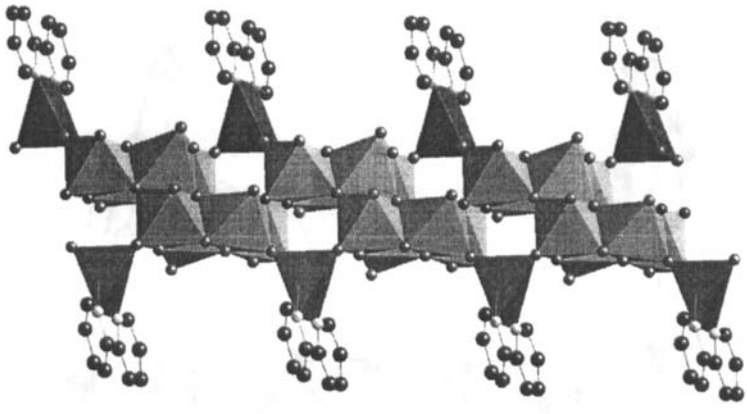

FIGURE 8 The structure of $[\{Cu(2,2'\text{-bpy})\}_2Mo_8O_{26}]$ (**5**). The fusion sites of he δ–$[Mo_8O_{26}]^{4-}$ motifs are highlighted

However, it is apparent that significant synergistic interactions between the molybdenum oxide component and the polymeric cations render the structural chemistry complex and unpredictable, rather than a simplistic "ship in the bottle" conceptualization. Three distinct subclasses of materials based on the molybdenum oxide submotif are emerging: (i) those exhibiting discrete oxomolybdate clusters; (ii) those in which the secondary metal site is directly incorporated into the molybdenum oxide substructure to produce a bimetallic oxide phase; and (iii) materials with distinct molybdenum oxide chains entrained within a cationic polymer framework.

Polymeric Cations and Molybdate Clusters

The structural prototype is provided by $[\{Cu(4,4'\text{-bpy})\}_4Mo_8O_{26}]$ (**6**),[16] shown in Figure 9. The structure is constructed from $\{Cu(I)(4,4'\text{-bpy})\}_n^{n+}$ chains and discrete δ–$[Mo_8O_{26}]^{4-}$ clusters. The cationic component provides a rigid scaffolding of two sets of chains oriented at right angles and containing digonally coordinated Cu(I) centers. The two sets of chains propagate so as to form cavities occupied by the polyoxomolybdate clusters. One set of cationic chains forms pairs of parallel, face to face rods. The Cu(I) sites of these double chains coordi-

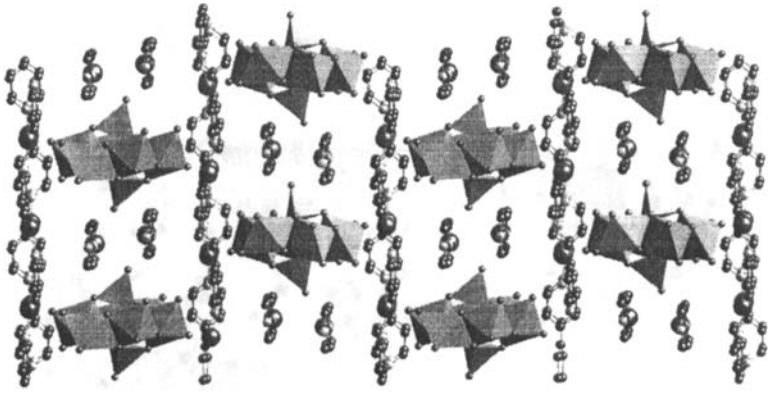

FIGURE 9 A view of the structure of $[\{Cu(4,4'\text{-bpy})\}_4Mo_8O_{26}]$ (**6**)

nate to the terminal oxo-groups of the molybdate clusters to provide a virtual layer structure in which the parallel $\{Cu(bpy)\}_n^{n+}$ double strands and the molybdate clusters are sandwiched between layers of parallel cationic chains which do not interact with the molybdate oxo-groups.

A structural variant is provided by $\{Cu(bpe)\}_4Mo_8O_{26}]$ (**7**),[30] shown in Figure 10. In contrast to the structure of **6**, the α-form of the octamolybdate is present. The molybdate subunits are linked through $\{Cu(bpe)\}_n^{n+}$ double chains into a two-dimensional network. While structure **7** shares with compound **6** the presence of interlamellar and non-interacting cationic chains, the chains of **7**run parallel to the double chain, rather than at right angles as in **6**.

The coordination polymer scaffolding may be modified by introducing a d-block site with different coordination preferences than those of Cu(I), such as Ni(II) which favors octahedral geometry. The unusual structure of $[\{Ni(4,4\text{-bpy})_2(H_2O)_2\}_2Mo_8O_{26}]$ (**8**)[16] illustrates this point and serves to reinforce the unpredictability of the architecture of these composite materials. As shown in Figure 11, the structure of **8** is constructed from ε-$[Mo_8O_{26}]^{4-}$ clusters and $\{Ni(bpy)_2(H_2O)_2\}_n^{2n+}$ one-dimensional zig-zag chains. This cationic component consists of *fac* $\{NiN_3O_3\}$ octahedra linked through bridging 4,4'-bpy ligands. Each Ni(II) site is consequently bonded to a nitrogen donor from each of three 4,4'-bpy ligands, two aqua ligands and an oxo-group of the molybdate

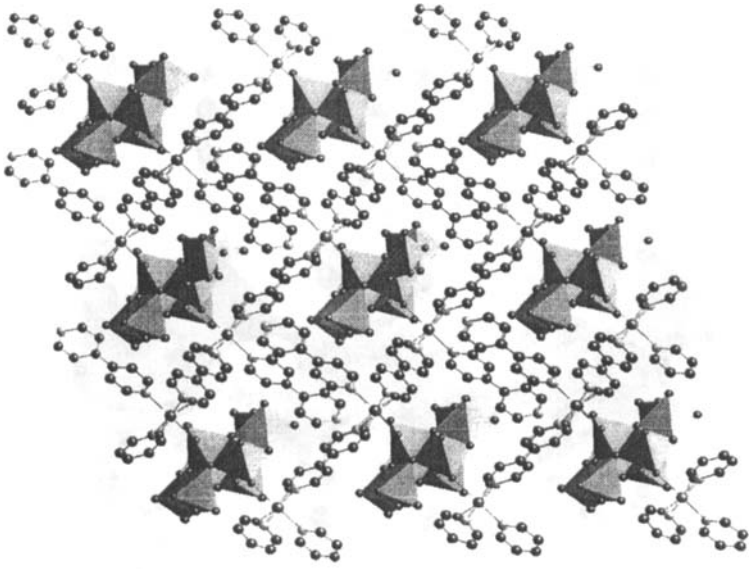

FIGURE 10 The two-dimensional network of $[\{Cu(bpe)\}_4Mo_8O_{26}]$ (**7**)

cluster. Since the bridging 4,4'-bpy ligands occupy *cis* positions on the nickel, the cationic chains exhibit a 90° fold at each nickel site. Curiously, the third bpy ligand on each Ni site is monodentate with a pendant arm oriented parallel to a similar pendant group from an adjacent polymeric chain.

The oxo-groups of a given molybdate cluster bond to nickel sites from adjacent chains to produce a two-dimensional covalently linked network.

Incorporation of the Secondary Metal into the Oxide Substructure: Bimetallic Oxide Phases

Compound **7** $[\{Cu(bpe)\}_4Mo_8O_{26}]$ was prepared under reducing conditions at low pH. When the reaction is carried out under oxidizing conditions, the Cu(II) phase $[Cu(bpe)(MoO_4)]$ (**9**)[31] s isolated. As shown in Figure 12, the structure may be described as $\{Cu(bpe)\}_n^{2n+}$ chains linked through bridging $\{MoO_4\}^{2-}$ tetrahedra into a three-dimensional

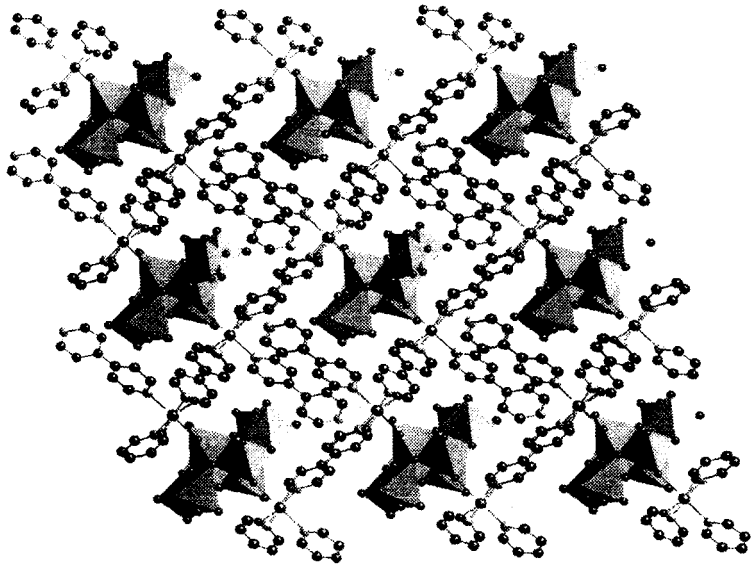

FIGURE 11 A view of the structure of $[\{Ni(4,4'\text{-bpy})_2(H_2O)_2\}_2Mo_8O_{26}]$(**8**)

framework. Alternatively, the structure may be viewed as bimetallic oxide layers $\{CuMoO_4\}$ with bridging bpe ligands occupying the interlamellar space. The layer is constructed from fused twelve-membered $\{Cu_3Mo_3O_6\}$ rings. The Cu(II) centers exhibit trigonal bipyramidal geometry $\{CuN_2O_3\}$; consequently, each copper center is bridged to three molybdenum sites in the layer.

That the geometry of the tethering unit may have a profound structural influence is illustrated by the structure of $[Cu(bpa)_{0.5}(MoO_4)]$ (**10**).[32] The bpa ligand may be distinguished from bpe not only by the relative tether lengths but also by the relative orientations of the nitrogen donor groups, which are parallel in bpe but angled at *ca.* 115° in bpa. The structural consequences are revealed in Figures 12 and 13. The structure of (**10**) consists of $\{CuMoO_4\}$ oxide layers linked by bpa ligands into a three-dimensional framework. In a similar fashion to [Cu(bpe) MoO_4], the structure of **10** displays the pattern of alternating organic-inorganic regions.

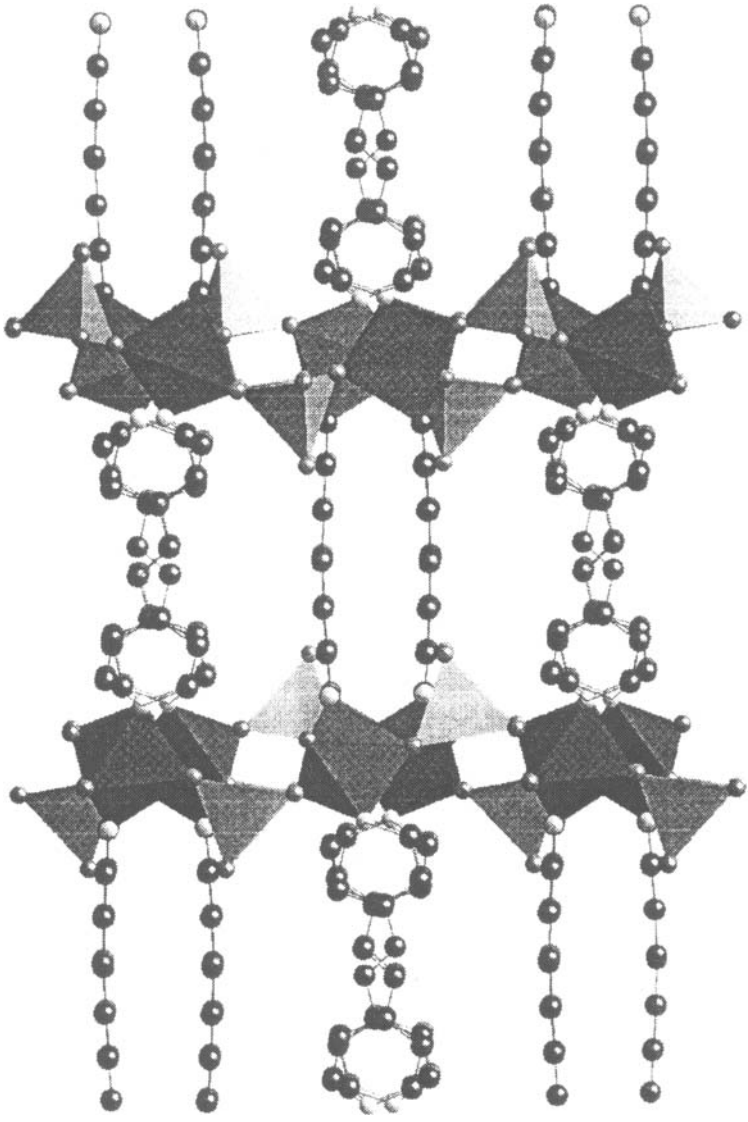

FIGURE 12 (a) The structure of [Cu(bpe)(MoO_4)](**9**)

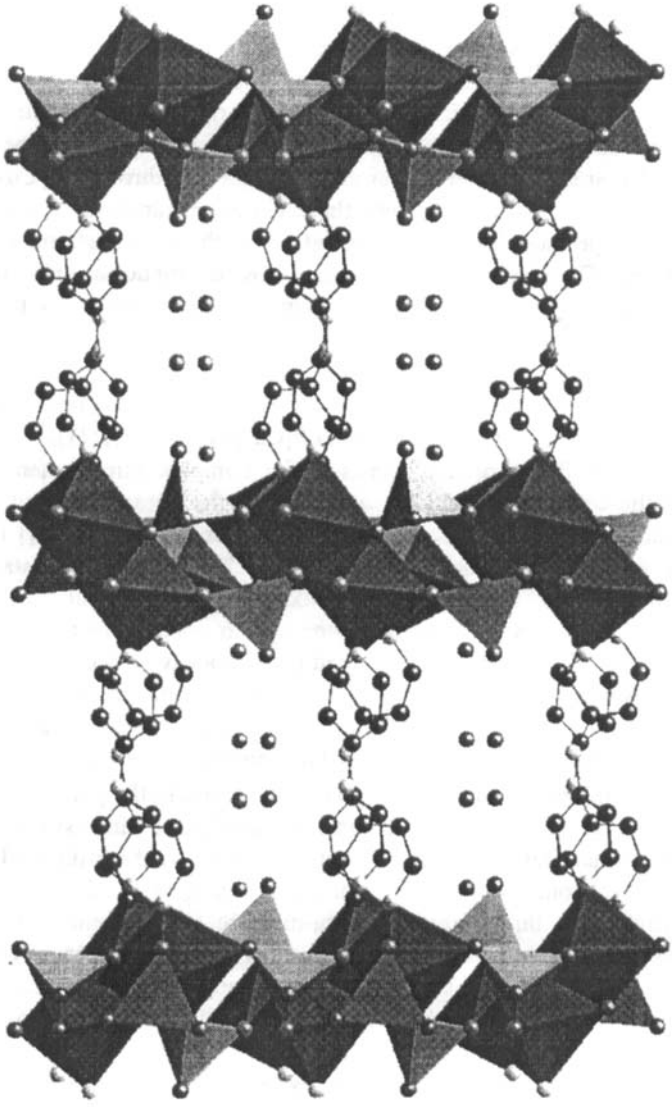

FIGURE 13 (a) A view of the structure of $[Cu(bpa)_{0.5}(MoO_4)]$ (**10**)

The inorganic layer is constructed from $\{MoO_4\}$ tetrahedra and $\{CuO_5N\}$ octahedra which form double chains linked through {Cu-O-Mo} bridges into a two-dimensional network. One Cu site forms corner-sharing interactions with five adjacent Mo sites of the chain, while the second Cu site forms four corner-sharing linkages to Mo chain sites and one to an Mo site of an adjacent chain. In addition, the two unique Cu sites form a binuclear edge-sharing unit through a $\{Cu_2O_2\}$ interaction. One Mo site bridges three Cu binuclear units of a given chain and provides linkage to an adjacent chain through its fourth oxo-group. The second Mo site bridges three Cu binuclear units of the chain and projects a terminal oxo-group into the interlamellar region. The contrasting layer structures of **9** and **10** are shown in Figure 14.

In order to assess the influence of significant donor group separation on structure, the pyrazine ligand was introduced into the copper-molybdate system, resulting in the isolation of $[Cu(pz)_{0.5}MoO_4]$ (**11**),[32] shown in Figure 15. The structure consists of a complex three-dimensional bimetallic oxide with channels occupied by the pyrazine ligand. The inorganic framework is constructed from corner-sharing $\{MoO_4\}$ tetrahedra and $\{CuO_4N\}$ square pyramids, which form chains of stacked $\{Cu_2Mo_2O_4\}$ rings. Each Mo site links three adjacent Cu sites of a chain and employs the fourth oxo-groups to connect to an adjacent chain. Four adjacent chains are linked to form a cavity occupied by the pyrazines which serve to ligate to Cu sites of opposite chains. The structure may be described as a $\{CuMoO_4\}$ three-dimensional framework providing channels occupied by organic templating molecules.

The pyrimidine ligand offers an obvious variant to the pyrazine component of **11** and results in an unanticipated three-dimensional copper-molybdate framework. The structure of $[Cu_2(pyrd)Mo_3O_{10}]$ (**12**) is constructed from $\{MoO_6\}$ octahedra and $\{CuO_3N\}$ tetrahedra, which link to form a three-dimensional bi-metallic oxide framework with channels occupied by the pyrimidine groups. As shown in Figure 16, the $\{MoO_6\}$ octahedra form a chain of edge-sharing polyhedra, structurally analogous to that observed for the one-dimensional $(NH_4)_2[Mo_3O_{10}]$. Each Cu site coordinates to two oxo-groups of two Mo sites of one chain and bridges an adjacent chain by bonding to one oxo-group. In addition, each Cu center coordinates to a nitrogen donor of a pyrimidine ligand, which serves to bridge to a second Cu site through its second nitrogen donor. When viewed along the crystallographic *a* axis, the Mo-oxide chains are linked through stacked $\{CuO_3N\}$ tetrahedra to pro-

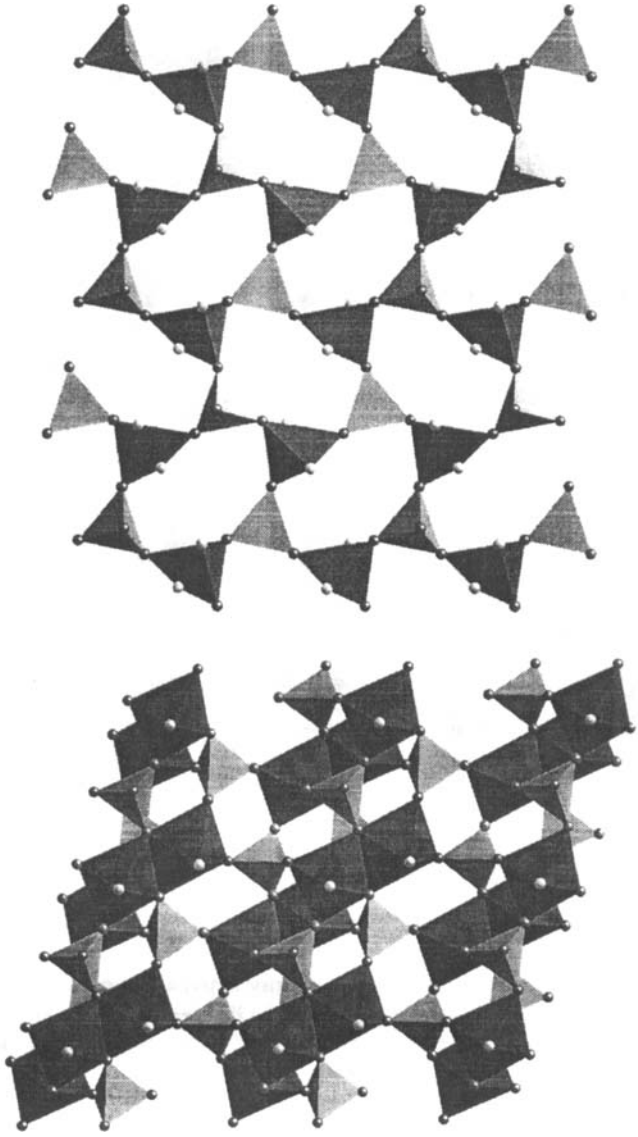

FIGURE 14 Polyhedral representations of the $\{CuMoO_4\}$ layers of (a) $[Cu(bpe)MoO_4]$ (**9**) and (b) $[Cu(bpa)_{0.5}(MoO_4)]$(**10**)

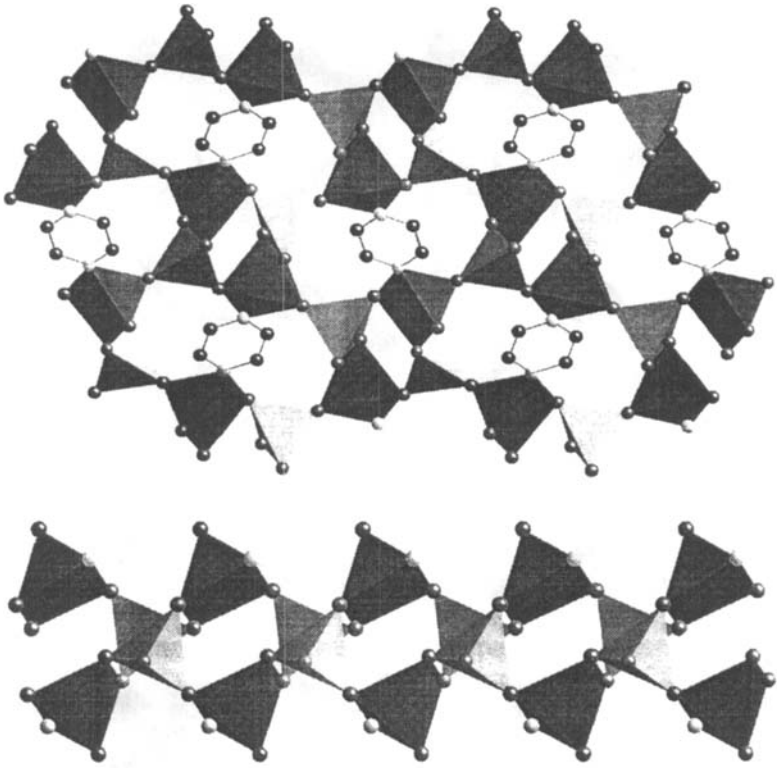

FIGURE 15 (a) A view of the structure of $[Cu(pz)_{0.5}(MoO_4)]$ (**11**), showing the channels occupied by the pyrazine ligands; (b) A view of one copper-molybdate chain

duce channels of sufficient diameter to accommodate parallel stacks of pyrimidine groups.

The third member of the $C_4H_4N_2$ family is pyridazine. The influences of donor group geometry are dramatically illustrated by the structure of $[\{Cu(pyridazine)\}_4Mo_8O_{26}]$ (**13**),[30] shown in Figure 17. A number of significant differences between the structure of **13** and those of **11** and **12** may be identified. The pyridazine derivative contains reduced copper rather than Cu(II) as in **11** and **12**. No Cu(II) derivative could be isolated in the presence of pyridazine which serves to reduce the Cu(II) starting material to Cu(I). In contrast to structures **11** and **12**, that of **13** contains

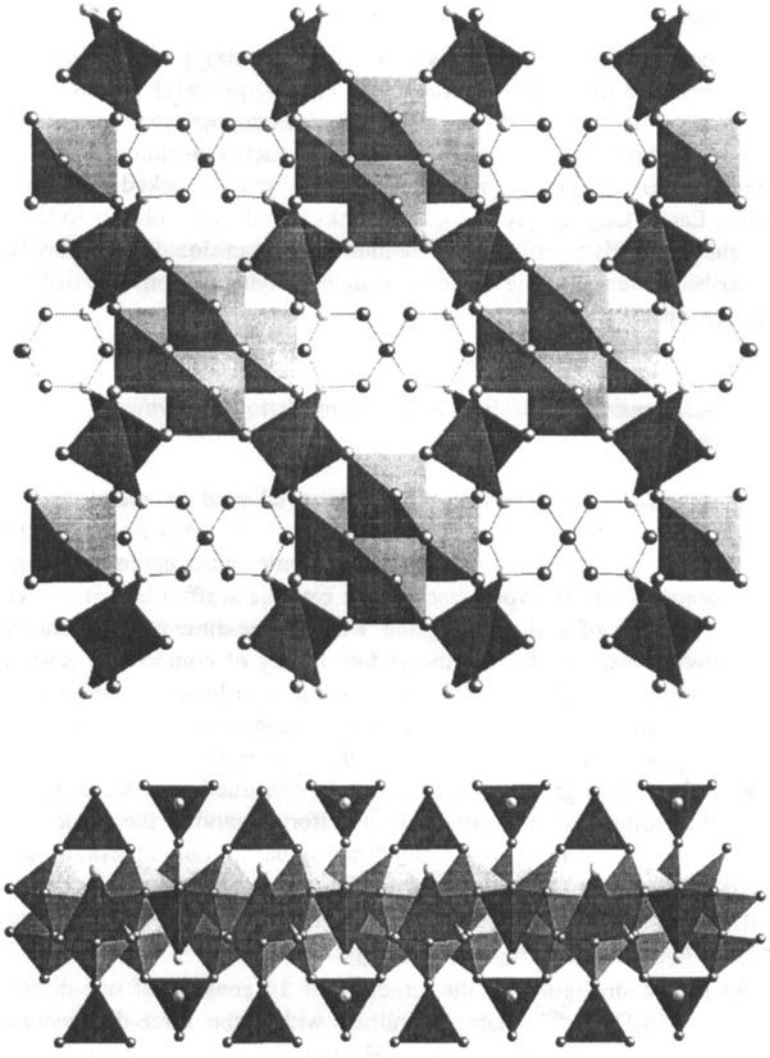

FIGURE 16 (a) The structure of $[Cu_2(pyrimidine)Mo_3O_{10}]$ (**12**), showing the three-dimensional copper-molybdate framework and the layer channels containing the pyrimidine ligands; (b) A view of an isolated molybdate chain decorated by copper sites which serve to link adjacent chains

discrete γ–molybdate clusters, rather than three-dimensional inorganic frameworks.

Each molybdate cluster bonds to four $\{Cu_2(pyrdz)_2\}$ units, which are present in the form of the tetranuclear $\{Cu_4O_6(pyrdz)_4\}$ clusters. The copper clusters consist of pairs of oxo-bridged copper tetrahedra which are linked through four pyridazine ligands in such a fashion as to generate a Cu_4 box of dimensions 3.25 Å × 3.02 Å with π-stacked pyridazine rings. Each $\{Cu_4O_6(pyrdz)_4\}$ cluster links a molybdate cluster to three neighboring cluster units. The resultant two-dimensional sheet may be described in terms of the corner-sharing of polyhedra from two distinct cluster types.

Three-Dimensional Coordination Complex Cationic Polymer Frameworks

Exploitation of the diversity of topologies adopted by metal-dipodal organonitrogen ligand complexes has provided a strategy for modifying the structures of molybdenum oxide anionic substructures through incorporation into the void space of the cationic scaffolding. However, in no instance of a dipodal ligand was a three-dimensional cationic framework observed for the molybdate family of composites, despite introduction of M^{2+} sites with octahedral coordination preferences. Recent studies on crystal engineering of three-dimensional frameworks provide precedent for the use of tripodal or higher denticity ligands with appropriate donor group orientations in the construction of architectures with three-dimensional motifs.[33] In an effort to modify the oxide substructure by providing a rigid three-dimensional cationic matrix, a "ship in the bottle" approach, the riazolate ligand was adopted as a linker for Cu^{2+} sites in the framework construction, providing the unusual material $[\{Cu_2(triazolate)_2(H_2O)_2\}Mo_4O_{13}]$ (**14**).[34]

As shown in Figure 18, the structure of **14** consists of one-dimensional $\{Mo_4O_{13}\}_n^{2n-}$ chains entrained within the three-dimensional framework of the $\{Cu_2(triazolate)_2(H_2O)_2\}_n^{2n+}$ polymeric coordination cation. There are two unique copper sites in the cationic framework. One site Cu(A) is effectively square pyramidal $\{CuN_4O\}$ through ligation to four triazolate nitrogen donors, one from each of four triazolate ligands and to a terminal oxo-group of the molybdate chain. The second site Cu(B) is octahedral $\{CuN_2O_4\}$, exhibiting coordination to two *trans*

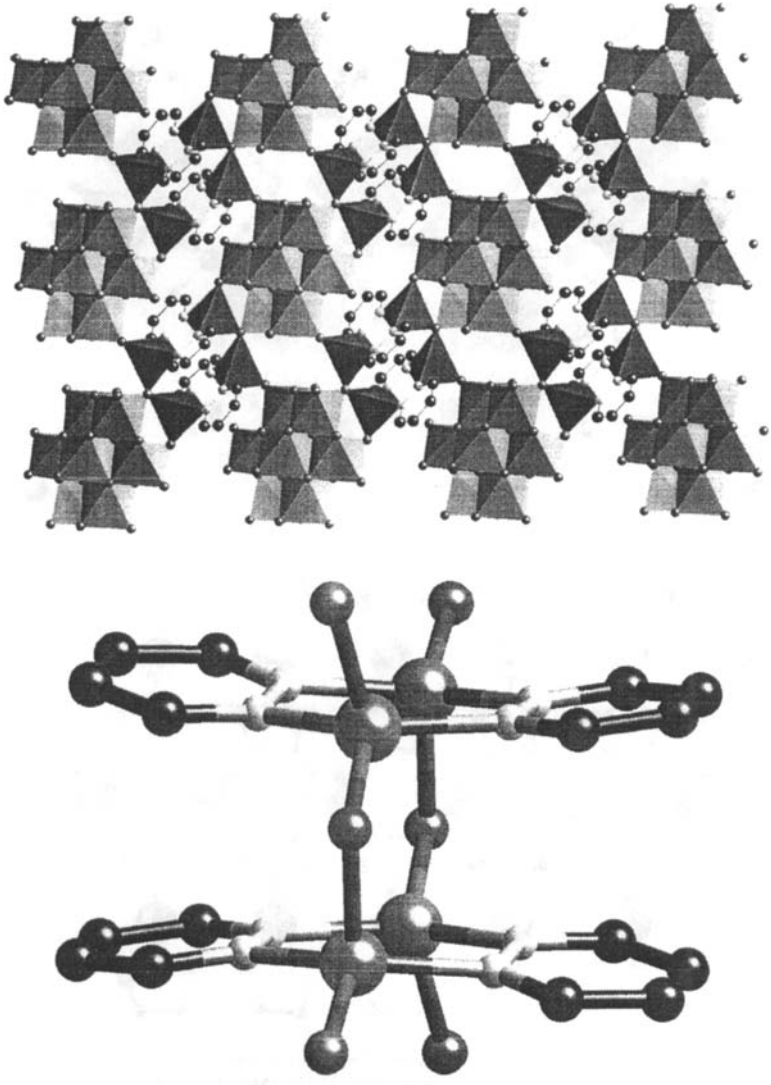

FIGURE 17 (a) The interactions between the γ-$[Mo_8O_{26}]^{4-}$ units and $\{Cu_2(pyridazine)_2\}^{2+}$ cations of $[\{Cu(pyridazine)\}_4Mo_8O_{26}]$ (**13**) to produce a tessellated notif; (b) The $\{Cu_4(pyridazine)_4O_6\}^{8+}$ cluster of (**13**)

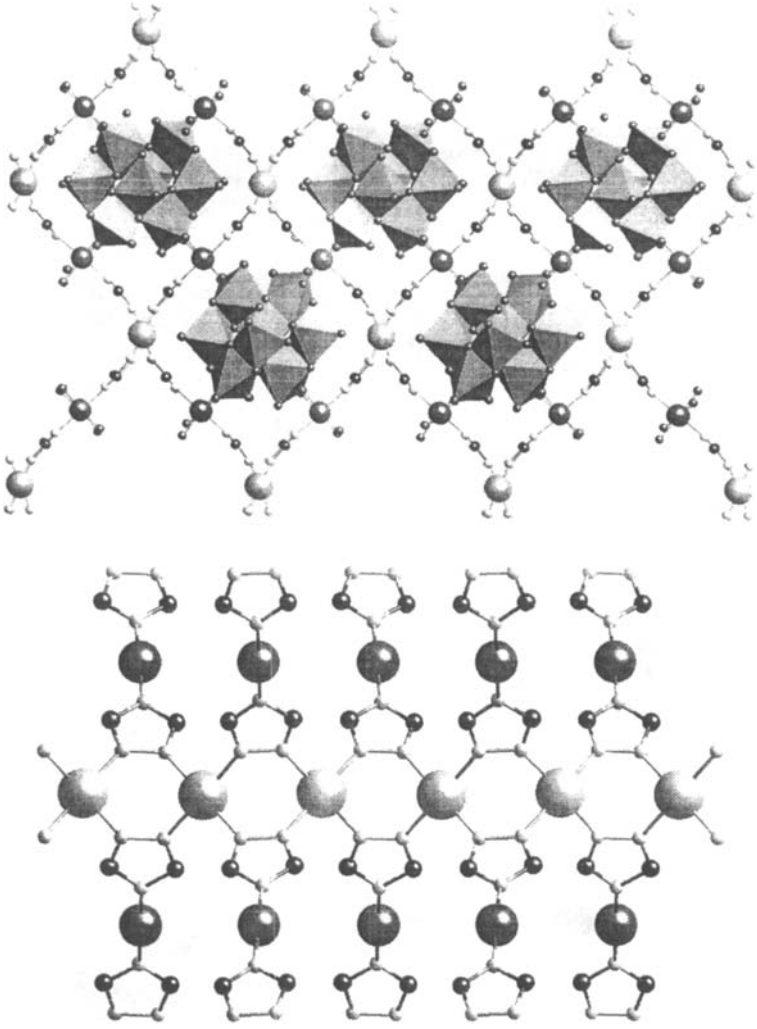

FIGURE 18 (a) A view parallel to the crystallographic *b* axis and to the molybdenum oxide chain of the structure of $[\{Cu_2(triazolate)_2(H_2O)_2\}Mo_4O_{13}]$ (**14**). The molybdate chain is depicted in polyhedral form. The large lighter spheres are the Cu(A) sites, the smaller darker spheres are the Cu(B) sites. (b) A view parallel to the crystallographic *a* axis of the chain formed by triazolate bridged Cu(A) sites (large, lighter spheres) and the linkage through Cu(B) centers(smaller, darker spheres) to adjacent chains

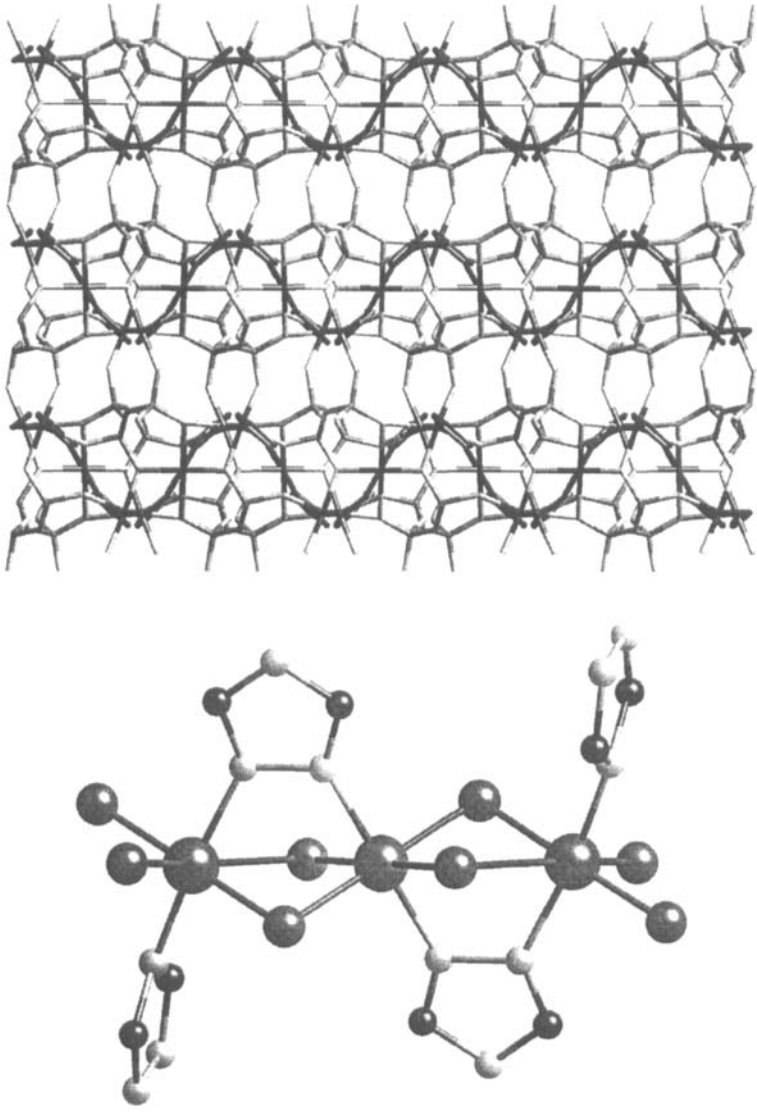

FIGURE 19 (a) A view parallel to the [001] direction of the structure of [{Cu_3(triazolate)$_2$}V_4O_{12}] (**15**). (b) The trinuclear motif from which the network is constructed, showing also the coordination to the oxo-groups of the vanadate chains

disposed triazolate nitrogen donors, two aquo ligands, and two terminal oxo-groups of the molybdate chains. The organic moiety adopts the anionic triazolate form in a three connect ligation mode. The resulting cationic framework is constructed from undulating chains of Cu(A) sites bridged through the 1,2-nitrogen donors of the triazolate ligands and linked to the adjacent chains through the Cu(B) centers which coordinate to the remaining ^{4}N- donors of the triazolate ligands. This connectivity pattern produces a honeycomb network when viewed along the crystallographic *c* axis. Furthermore, the disposition of bridging triazolate ligands about a chain results in linkage to four adjacent parallel chains, giving rise to large tunnels which are occupied by the molybdate chains. The undulating molybdate chain is constructed from edge-sharing molybdenum octahedra and tetrahedra.

While the concept of "ship in the bottle" synthesis of oxides is attractive from the viewpoint of designed crystalline materials, it naively neglects the consequences of interactions between the secondary metal M^{2+} site and the molybdenum oxide component. The elaboration of the chemistry of these composites establishes that the oxide is not simply clay to be molded within a rigid cationic substructure, but rather a synergistically active component of the composite, a feature illustrated by the structure of $[\{Cu_3(triazolate)_2\}V_4O_{12}]$ (**15**).[35]

As shown in Figure 19, the structure of **15** consists of a three-dimensional covalent framework constructed from two-dimensional $\{Cu_3(triazolate)_2\}_n^{4n+}$ networks linked through one-dimensional $\{VO_3\}_n^{n-}$ chains. The cationic network when viewed parallel to [001] displays a pronounced sinusoidal ruffling with an amplitude of about 4.75Å and a period of 8.87Å. The layers are composed of Cu(II) sites digonally coordinated through triazolate ligands, each of which bridges three copper sites. Within each layer, there are large rhombic rings, $\{Cu_6(triazolate)_6\}$, which form the distinctive lattice work motif with each ring sharing an edge with six adjacent rings. The $\{VO_3\}_n^{n-}$ linear chains nestle in the troughs formed by the ruffling of the layers. The copper sites of the network are covalently bound to the terminal oxo-group of the vanadate chains so as to give distorted octahedral 4+2 $\{CuN_2O_4\}$ geometry at each copper site. This connectivity pattern results in oxo- and triazolato-bridged trinuclear units, each of which bridges through triazolate ligands to four adjacent trinuclear units in forming the two-dimensional network. The folding of the copper-triazolate sheet is a consequence of the relative orientations of the triazolate ligands, which

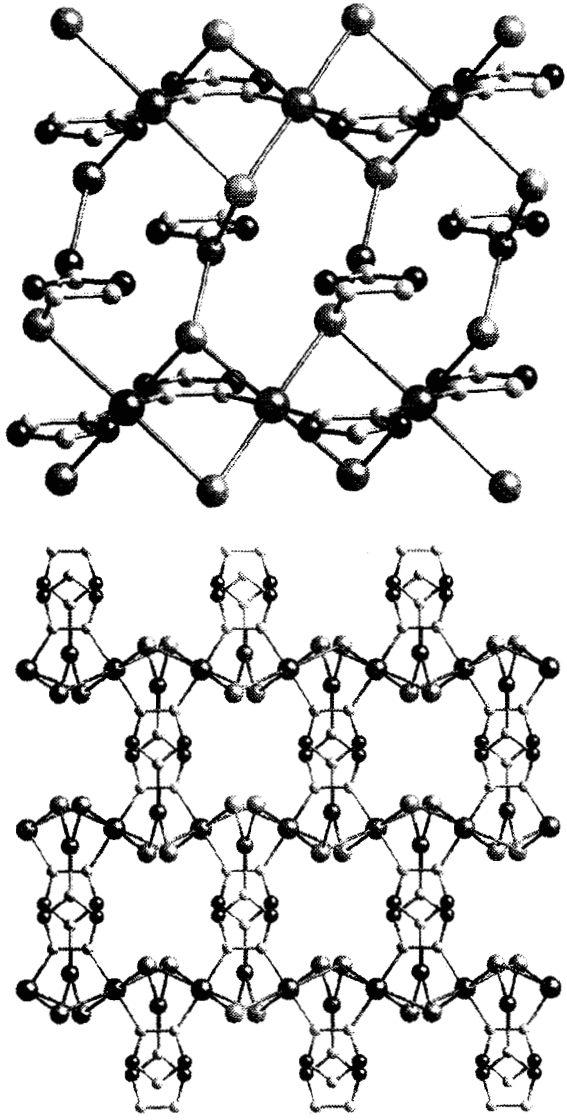

FIGURE 20 (a) The two-dimensional network of [Cu_2Br_2(triazolate)] (**16**). (b) A view of the three-dimensional structure of **16**, showing the linking of $\{Cu_2Br_2\}_n^{n+}$ layers through triazolate ligands

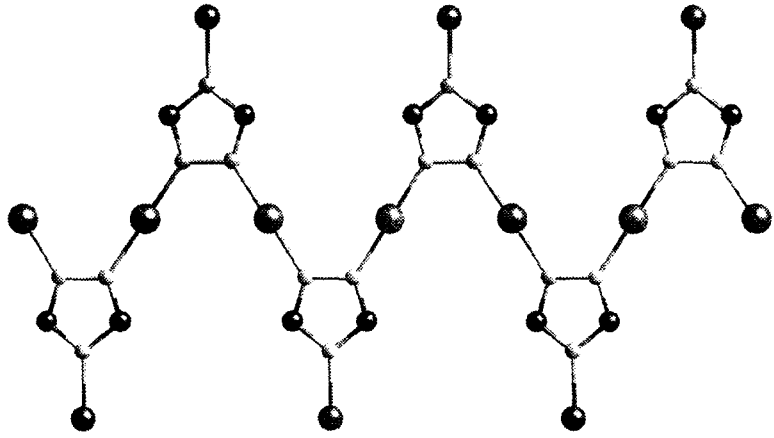

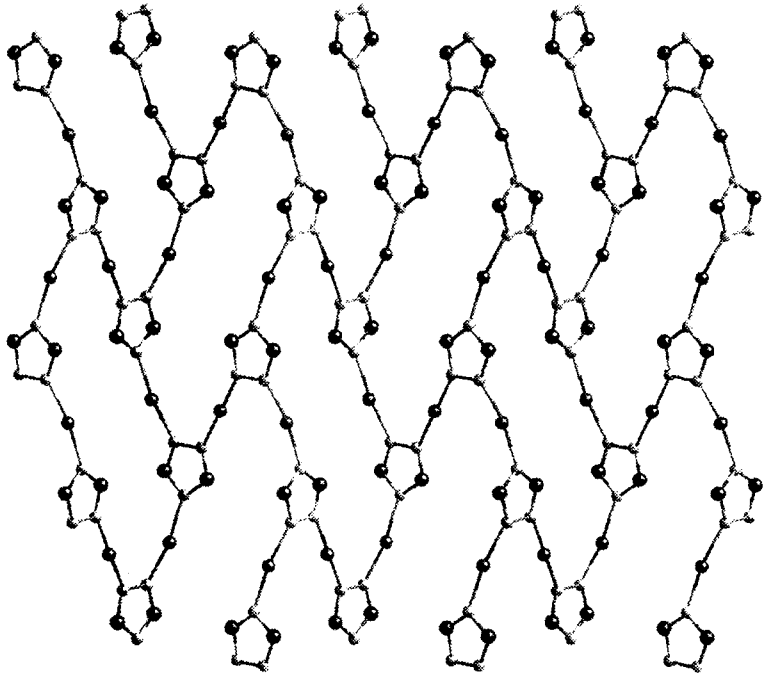

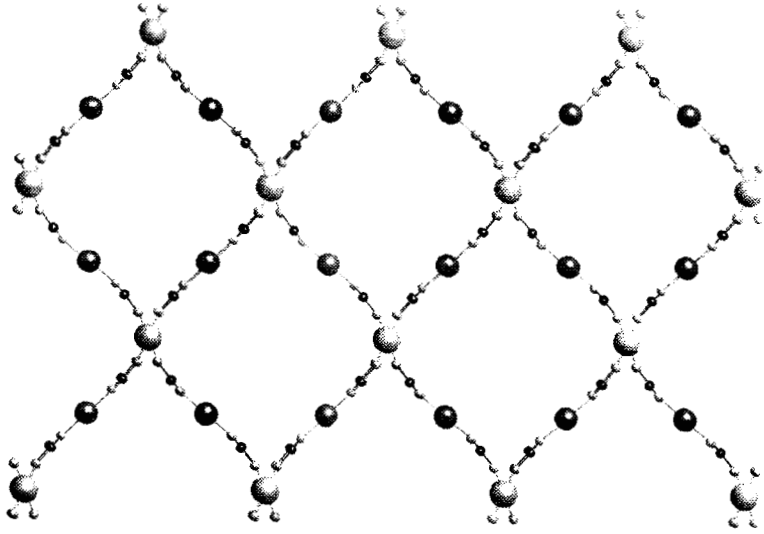

FIGURE 21 The one-, two-, and three-dimensional Cu-triazolate cationic substructure of **16, 15**, and **14**, respectively

alternate in pairs with parallel and perpendicular ring planes. The vanadate chains which occupy the folds of the copper-triazolate layers consist of corner-sharing vanadium tetrahedra.

Anion control of cationic substructure is further illustrated by adopting a halide as the charge-compensating component for the copper-triazolate cationic polymer, rather than a catenated metal oxide anion. The structure of $[Cu_2Br_2(triazolate)]$(**16**)[36] consists of a three-dimensional covalent framework constructed from Cu^{2+}- and Cu^{1+}-halide-ligand substructures. As shown in Figure 20, the structure of **16** is constructed of one-dimensional $\{Cu(triazolate)Br_2\}_n^{n-}$ chains linked through Cu^{+1} centers into a three-dimensional framework. The Cu^{+2} sites exhibit six coordinate $\{CuN_2Br_4\}$ geometry through bonding to the 1,2-nitrogen donors of the bridging triazolate groups and to the bridging halide ligands. Each bromine site is three-coordinate and serves to bridge two Cu^{2+} sites of a chain to a Cu^{+1} site. The Cu^{+1} sites display trigonal planar $\{CuNBr_2\}$ geometry and provide the hinges which bridge the $\{Cu(triazolate)Br_2\}_n^{n-}$ chains into the framework structure of **16**. Thus,

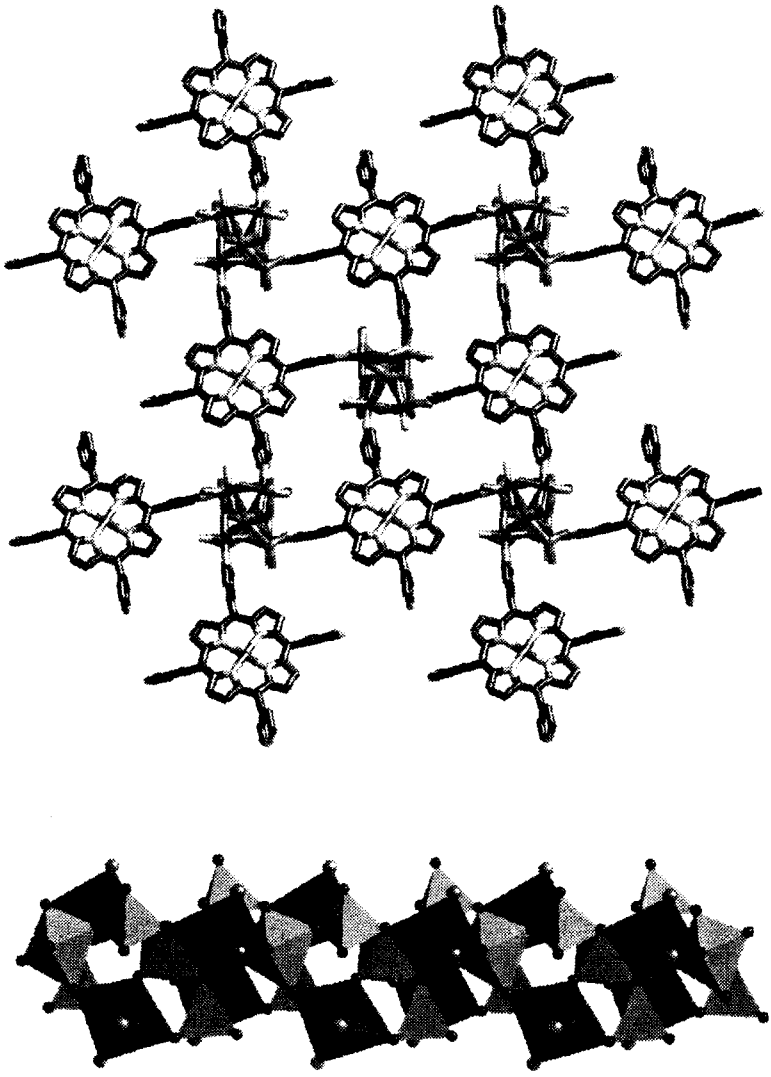

FIGURE 22 (a) A view of the structure of [{Cu(tpypor)}$Cu_2Mo_3O_{11}$](**17**), illustrating a metal oxide linked metal-porphyrin network. (b) A view of the bimetallic {$Cu_2Mo_3O_{11}$} chain

each Cu^{1+} center bonds to bromide units from adjacent Cu^{2+}, chains to produce a two-dimensional substructure. Furthermore, each Cu^{1+} site bonds to the 4-nitrogen donor of a triazolate ligand from a chain of an adjacent layer.

The role of the anion in self-assembly of the composite materials **14–16** is most dramatically illustrated in Figure 21, which shows the {Cu(triazolate)} cationic skeletons of the structures, stripped of the charge-compensating and coordinating anionic components. The one-, two- and three-dimensional cationic motifs observed for **16, 15**, and **14**, respectively, illustrate the importance of the synergistic interactions between the cationic and anionic substructures of these composite materials.

Multifunctional Ligands for the Design of Cationic Substructures

Functionality is generally related to structural complexity. Appropriate ligands should allow the design of solids exhibiting the appropriate juxtaposition of metal sites for reactivity and cooperative electronic effects. One approach to such structural complexity exploits multifunctional ligands, for example, one capable of bridging metal sites while also providing a functional center. Tetrapyridylporphyrin provides an example of a complex ligand capable of four-fold connectivity and providing a porphyrin site for additional coordination and functionality. The first example of a three-dimensional framework material constructed from metal oxide and porphyrin subunits is provided by [{Cu(tpypor)}$Cu_2Mo_3O_{11}$] (**17**),[37] shown in Figure 22. The structure of **17** consists of a tesselated porphyrin network[38] linked into a three-dimensional framework through bimetallic oxide chains. One copper site is bound to the nitrogen donors of the porphyrin while the second copper site exhibits its octahedral $\{CuN_2O_4\}$ geometry through bonding to two pyridyl donors from two tpypor ligands and to four oxygen ligands from the molybdate chain. The molybdate substructure consists of a chain of corner-sharing octahedra and tetrahedra. Each $\{MoO_6\}$ octahedron is linked to its neighbors through doubly-bridging $\{MoO_4\}$ tetrahedra and is decorated with a terminal $\{MoO_4\}$ tetrahedron. This unusual molybdate chain is linked through terminal oxo-groups to the pyridyl ligated copper sites to form a neutral bimetallic $\{CuMo_3O_{11}\}$ chain.

The role of the secondary metal site in determining structure is illustrated by the structure of [Fe_2(tpypor)Mo_6O_{19}] (**18**)[35] shown in

Figure 23. The structure consists of a three-dimensional cationic framework $\{Fe_2(tpypor)\}_n^{2n+}$ and isolated $[Mo_6O_{19}]^{2-}$ clusters as charge-compensating and space-filling subunits.

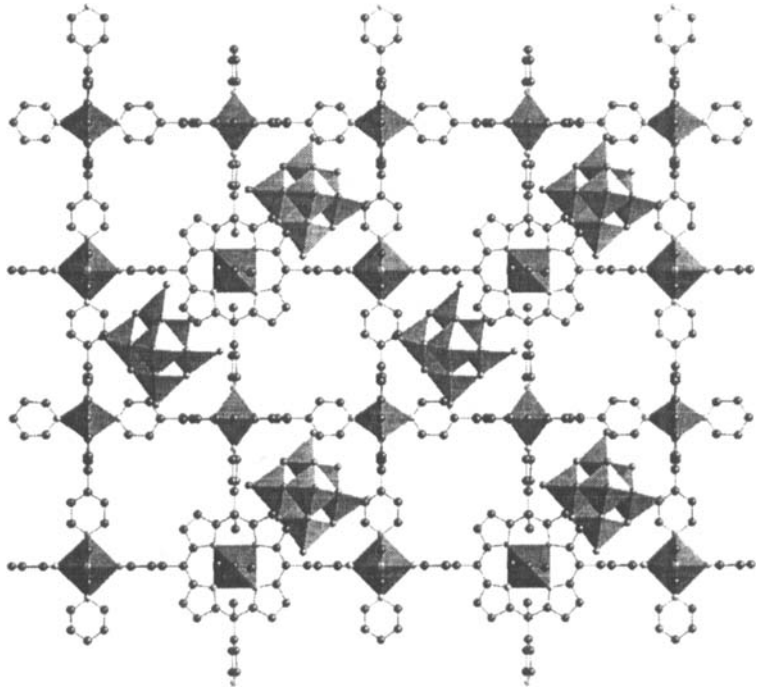

FIGURE 23 A view of the structure of $[Fe_2(tpypor)Mo_6O_{19}]$(**18**)

CONCLUSIONS

Organonitrogen templated molybdenum oxides represent a new class of materials in which an organic component exerts a crucial role in dictating the inorganic oxide microstructure. The organic component may manifest a variety of structural roles, including templating, tethering of functional groups, passivation of metal coordination spheres to yield low dimensionality materials, ligand to secondary metal centers, and linker for additional complex functional groups.

This synthetic approach to new solid phase molybdenum oxides occupies the interface between materials science and coordination chemistry. The emerging theme focuses on the association of an organic component, acting as a ligand, tether, or structure directing moiety, with the inorganic framework of the solid to provide unique composites. While some organic components may limit the size of inorganic cluster subunits of a solid by passivating the surface of an aggregate through capping, such ligands may also serve to link inorganic subunits into complex networks.

Most significantly, the chemistry of these molybdenum oxide-secondary metal organonitrogen hybrids belies the naïve "ship in the bottle" construct, wherein the engineered cationic substructure provides a rigid matrix for the isolation of the metal oxide motif; but rather the observations suggest a synergism between the oxide and cationic coordination complex polymer at the organic-inorganic interface. However, while the approach of introducing the appropriate metal cation and ligand to accomplish the self-assembly of a polymeric cationic substructure has allowed a more or less predictable approach to the isolation of low dimensional oxide subunits, absolute synthetic control in the sense of crystal engineering remains elusive. Of course, these composite materials are metastable phases, crystallizing under non-equilibrium conditions from a complex hydrothermal domain. We are currently exploring the use of preformed cationic networks and frameworks and of oxide clusters and the exploitation non-hydrothermal conditions as synthetic approaches.

Acknowledgements

This work was supported by a grant from the National Science Foundation, CHE9617232.

References

1. A. J. Cheetham, Science **264**, 794 (1994) and references therein.
2. D. W. Bruce, D. O'Hare, eds., Inorganic Materials, Wiley, Chickester (1992).
3. T. G. Reynolds, R. C. Buchanan, Ceramic Materials for Electronics **2nd ed.**, R. C. Buchanan, ed., Dekker, New York, 207 (1991).
4. W. Büchner, R. Schliebs, G. Winter, K. H. Büchel, Industrial Inorganic Chemistry, VCH, New York (1989).
5. W. H. McCarroll, Encyclopedia of Inorganic Chemistry **vol. 6**, R. B. King, ed., John Wiley and Sons, New York, 2903 (1994).

6. G. H. Hartling, Ceramic Materials for Electronics **2nd ed.**, R. C. Buchanan, ed., Dekker, New York, 129(1991).
7. D. I. Makin, Modern Oxide Materials, B. Cockayne and D. W. Jones, eds., Academic Press, New York, 235 (1972).
8. B. Mason, Principles of Geochemistry **3rd ed.**, Wiley, New York (1966).
9. L. L. Hench, Inorganic Biomaterials, in Materials Chemistry, An Emerging Discipline, **ACS Series 245**, L. V. Interrante, L. A. Casper, A-B Ellis, 523–547 (1995).
10. S. Mann, J. Chem. Soc., Dalton Trans., 3953 (1997).
11. A. Rabenau, Angew. Chem., Int. Ed. Engl., **24**, 1026 (1985).
12. (a) R. C. Haushalter, L.A. Mundi, Chem. Mater, **88**, 149 (1988).
(b) M. L. Occelli, H. C. Robson, Zeolite Synthesis, American Chemical Society, Washington, D. C. (1989).
13. S. Mann, Nature, **365**, 499 (1993).
14. C. T. Kresge, M. E. Leonowicz, W. J. Roth, J. C. Vartuli, J. S. Beck, Nature, **359**, 710 (1992).
15. (c) R. C. Haushalter, L. A. Mundi, Chem. Mater., **4**, 31 (1992).
(d) M. I. Khan, L. M. Meyer, R. C. Haushalter, C. L. Schweitzer, J. A. Zubieta, J. L. Dye, Chem. Mater., **8**, 43 (1996).
16. D. Hagrman, C. Zubieta, D. J. Rose, J. Zubieta, R. C. Haushalter, Angew. Chem., Int. Ed. Engl., **36**, 873 (1997) and references therein.
17. D. Hagrman, P. Zapf, J. Zubieta, Angew. Chem. Int. Ed. Engl., **38**, 0000 (1999).
18. J. Gopalakrishnan, Chem. Mater., **7**, 1265 (1995).
19. M. I. Khan, J. Zubieta, Progr. Inorg. Chem., **43**, 1 (1995).
20. For a review of various frameworks and interpenetrating motifs see S. R. Batten, R. Robson, Angew. Chem., Int. Ed. Engl., **37**, 1460 (1998).
21. P. J. Zapf, J. Zubieta, unpublished results.
22. J. R. D. DeBord, R. C. Haushalter, L. M. Meyer, D. J. Rose, P. J. Zapf, J. Zubieta, Inorg. Chim. Acta, **256**, 165(1997).
23. M. T. Pope, Heteropoly and Isopoly Oxometalates, Springer, New York (1983).
24. M. Inoue, T. Yamase, Bull. Chem. Soc. Jpn., **68**, 3055 (1995).
25. R. Xi, B. Wang, K. Isobe, T. Nishioka, K. Toriumi, Y. Ozawa, Inorg. Chem., **33**, 833, (1994).
26. P. J. Zapf, C. J. Warren, R. C. Haushalter, J. Zubieta, Chem. Commun., 1543 (1997).
27. D. Hagrman, P. J. Zapf, J. Zubieta, Chem. Commun., 1283 (1998).
28. P. J. Zapf, D. Hagrman, J. Zubieta, unpublished results.
29. See for example:
(a) B. F. Abrahams, B. F. Hoskins, D. Michail, R. Robson, Nature, **369**, 727 (1994).
(b) R. Robson, Comprehensive Supramolecular Chemistry, **vol. 6**, J. L. Atwood, J. E. D. Davies, D. D. MacNicol, F. Vögtle, J.-M. Lehn, eds., Pergamon, New York, 733 (1996).
(c) M. J. Zaworotko, Chem. Soc. Rev., 283 (1994).
(d) M. Fujita, Y. J. Kwon, S. Washiza, K. Ogura, J. Am. Chem. Soc., **116**, 1151(1994).
(e) L. Carlucci, G. Ciani, D. M. Proserpio, A. Sironi, Inorg. Chem., **36**, 1736 (1997).
(f) L. Carlucci, G. Ciani, D. W. v. Gudenberg, D. M. Proserpio, A. Sironi, Chem. Commun., 631 (1997).
(g) L. Carlucci, G. Ciani, D. W. v. Gudenberg, D. M. Proserpio, Inorg. Chem., **36**, 3812 (1997).
(h) T. L. Hennigar, D. C. MacQuarie, P. Losier, R. D. Rogers, M. J. Zaworotko, Angew. Chem., Int. Ed. Engl., **36**, 972 (1997).
(i) A. J. Blake, S. J. Hill, P. Hubberstey, W.-S. Li, J. Chem. Soc., Dalton Trans., 909 (1998).

(j) A. J. Blake, S. J. Hill, P. Hubberstey, W.-S. Li, J. Chem. Soc., Dalton Trans., 913 (1997).
(k) M. A. Withersby, A. J. Blake, N. R. Champness, P. Hubberstey, W.-S. Li, M. Schröder, Angew. Chem., Int. Ed. Engl., **36**, 2327 (1997).
(l) C. V. K. Sharma, S. T. Griffin, R. D. Rogers, Chem. Commun., 215 (1998).
30. D. Hagrman, C. Sangregorio, C. J. O'Connor, J. Zubieta, J. Chem. Soc., Dalton Trans., 3707 (1998).
31. D. Hagrman, R. C. Haushalter, J. Zubieta, Chem. Mater., **10**, 361 (1998).
32. D. Hagrman, C. J. Warren, R. C. Haushalter, R. S. Rarig, Jr., K. M. Johnson III, R. L. LaDuca, Jr., J. Zubieta, Chem. Mater., **10**, 2091 (1998).
33. See for example: B. F. Hoskins, R. Robson, D. A. Slizys, Angew. Chem., Int. Ed. Engl., **36**, 2752 (1997).
34. D. Hagrman, J. Zubieta, Chem. Commun., 2005 (1998).
35. P. J. Zapf, J. Zubieta, J. Chem. Soc., Dalton Trans., in press.
36. R. Hammond, J. Zubieta, unpublished results.
37. D. Hagrman, P.J. Hagrman, J. Zubieta, Angew. Chem., in press.
38. C. M. Drain, F. Nifiates, A. Vasenko, J. D. Batteas, Angew. Chem., Int. Ed. Engl., **37**, 2344 (1998).